LA-UR-81-1555

TITLE: THE NUCLEAR EQUATION OF STATE STUDIED WITH HIGH-ENERGY HEAVY IONS

AUTHOR(S): J. R. Nix and D. Strottman

SUBMITTED TO: Adriatic Europhysics Study Conference on Nuclear Physics Dynamics of Heavy-Ion Collisions, Hvar, Croatia, Yugoslavia, May 25-30, 1981

University of California

LOS ALAMOS SCIENTIFIC LABORATORY
Post Office Box 1663 Los Alamos, New Mexico 87545
An Affirmative Action/Equal Opportunity Employer

Form No. 836 R3
St. No. 2629
12/78

UNITED STATES
DEPARTMENT OF ENERGY
CONTRACT W-7405-ENG. 36

THE NUCLEAR EQUATION OF STATE STUDIED WITH HIGH-ENERGY HEAVY IONS

J. R. NIX*

Max-Planck-Institut für Kernphysik
D-6900 Heidelberg, Federal Republic of Germany

and

Theoretical Division, Los Alamos National Laboratory
Los Alamos, New Mexico 87545

and

D. STROTTMAN

Theoretical Division, Los Alamos National Laboratory
Los Alamos, New Mexico 87545

Contents

*Alexander von Humboldt Senior U.S. Scientist Awardee.

J. R. NIX AND D. STROTTMAN

1. Introduction

We entered a new era in nuclear physics a few years ago. We had previously studied nuclei by bombarding them either with light projectiles or with heavy ions at low energy. Under these conditions, the nuclear density remains close to its equilibrium value and the excitation energy is relatively low. However, the development of accelerators that can accelerate heavy nuclei to relativistic energies has made it possible to begin to explore what happens when nuclei become highly compressed and excited.

Such studies permit us in principle to learn about the nuclear equation of state, the fundamental relationship specifying how the pressure depends upon density and thermal energy. At present we have experimental information about this important function only in the vicinity of the equilibrium ground state. However, theoretical speculations suggest that it may be extremely complicated, with nuclear matter undergoing one or more phase transitions as its density is increased.

In order for us to achieve our objective of learning about the nuclear equation of state from comparisons with experimental data, two important conditions must be realized in practice. First, high-energy heavy-ion collisions must involve some degree of coherent collective flow rather than being merely a superposition of hadron-hadron collisions. Second, the calculated quantities that are experimentally measurable must show some sensitivity to the input equation of state. We pay particular attention to these points here within the framework of two different types of fluid-dynamics models. Although these models have their limitations, they have the strong virtue of dealing directly rather than indirectly with the function that we are interested in. Any many-body forces that may be present at high density can be taken into account automatically through their effect on the equation of state, whereas other approaches are currently limited to two-body forces.

We do not have space here to review the many contributions of other groups to the field, but instead concentrate on those aspects in which we have been directly involved, after first discussing our current knowledge and theoretical speculations concerning the nuclear equation of state in sect. 2. Conventional relativistic nuclear fluid dynamics, which is based on the assumption that the nucleon mean free path is zero and consequently neglects the interpenetration of the target and projectile upon contact, is discussed in sect. 3. Results of such calculations performed for three

different equations of state are compared in sect. 4 with experimental data for both all impact parameters and central collisions for the reaction $^{20}Ne + ^{238}U$ at a laboratory bombarding energy per nucleon of 393 MeV. These comparisons suggest that we need to take into account target and projectile interpenetration, which is done in sect. 5 on the basis of a two-fluid model. We conclude in sect. 6 with an assessment of the present status and our future prospects for determining the nuclear equation of state with high-energy heavy ions.

2. Nuclear Equation of State

A region of nuclear matter in local equilibrium can be described by an equation of state, which specifies how the pressure depends upon density and thermal energy. In the rest frame of the matter under consideration, the total internal energy per nucleon is

$$E(n,I) = E_0(n) + I \ , \tag{1}$$

where $E_0(n)$ is the ground-state energy per nucleon at nucleon number density n and I is the thermal energy per nucleon, which is itself a function of n and either the entropy per nucleon S or the temperature T. The pressure p is then given by[22]

$$p = n^2 \left.\frac{\partial E(n,I)}{\partial n}\right|_S = n^2 \frac{dE_0(n)}{dn} + n^2 \left.\frac{\partial I}{\partial n}\right|_S \ ,$$

so that it contains separate contributions from the compressional energy and the thermal energy.

We currently have three pieces of experimental information concerning the ground-state energy per nucleon $E_0(n)$. The value of the equilibrium energy per nucleon given by a recent semi-empirical nuclear mass formula is[1a]

$$E_0(n_0) = -15.99 \text{ MeV} \ ,$$

the value of the equilibrium density obtained from analyses of elastic electron scattering and microscopic calculations of nuclear density distributions is[9,18,21]

$$n_0 = 3/[4\pi(1.16\ \text{fm})^3] = 0.153\ \text{nucleons/fm}^3 ,$$

and the value of the nuclear compressibility coefficient deduced from nuclear giant-monopole resonances is[4]

$$K = 9n_0^2 \left.\frac{d^2E_0(n)}{dn^2}\right|_{n_0} = 210 \pm 30\ \text{MeV} .$$

Although unknown experimentally at higher densities, theoretical speculations suggest that $E_0(n)$ may involve one or more phase transitions, as illustrated[22] in fig. 1. For example, doubling the nuclear density from its normal value could lead to a pion condensate, or a state containing a large number of bound pions.[5,11,13,14] Compression to several times normal density could result in a density isomer, or a quasistable state existing at other than normal density.[14,16,24] Still further compression could produce quark matter, in which the quarks that comprise nucleons become free.[3,7,15] To determine whether or not any of these phase transitions actually exist in nuclei is the exciting challenge that we face!

The thermal contribution to the pressure can be written as[22]

$$P_{\text{thermal}} = n^2 \left.\frac{\partial I}{\partial n}\right|_S = bnI ,$$

where b is in general a function of both n and I. However, b becomes especially simple in certain limiting cases. In the nonrelativistic Fermi-gas model

$$b = 2/3 , \qquad (7)$$

reflecting the proportionality of the thermal energy per nucleon to $n^{2/3}$. When the effect of interactions between the nucleons is taken into account

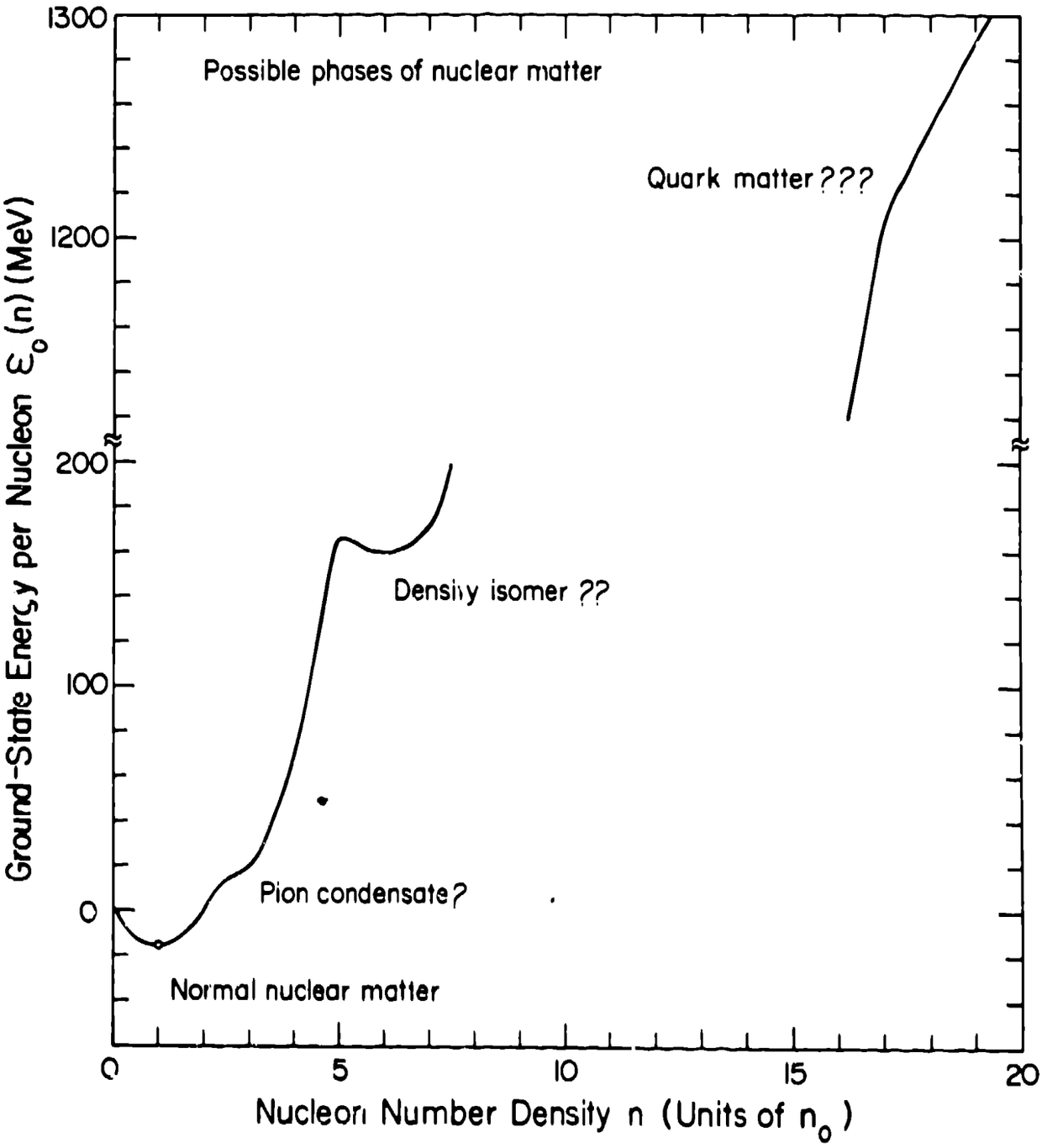

Fig. 1. Schematic illustration of three possible phase transitions in nuclear matter with increasing density.

by means of a density-dependent effective mass $m_{eff}(n)$, this result generalizes to[28]

$$b = \frac{2}{3} - \frac{d \ln m_{eff}(n)}{d \ln n} .$$

When mesons or other particles are produced, this result at high temperatures generalizes to

$$b = 2/(3 + N_m) ,$$

where N_m is the number of mesonic and other degrees of freedom that are excited per nucleon. Finally, in the ultrarelativistic Fermi-gas model with constant effective mass and no particle production

$$b = 1/3 .$$

To study the sensitivity of the calculated results to the input equation of state, we use the Fermi-gas result (2) for the thermal pressure and the three curves[23] shown in fig. 2 for the ground-state energy per nucleon $E_0(n)$. The solid line shows the result for a conventional nuclear equation of state with compressibility coefficient K = 200 MeV, and the dashed line shows the effect of doubling the compressibility coefficient to 400 MeV. The dot-dashed curve in fig. 2 shows the result for an equation of state with a density isomer at a density that is three times normal nuclear density, with an energy 2 MeV higher than at normal density and with the same curvature. This curve is qualitatively similar to some that have been computed numerically by Hecking and Weise,[11] who showed that pion condensation leads to a density isomer for certain values of their parameters.

For each of the three curves in fig. 2, we use the value $E_0(n_0) = -8$ MeV to simulate the effects of surface and Coulomb energies for finite nuclei and an older value[20] of $n_0 = 0.145$ nucleons/fm^3 for normal nucleon number density. The curves are calculated from a new functional form[21] which has the property that the speed of sound approaches the speed of light in the limit of infinite compression. This is achieved by parameterizing $E_0(n)$ for n greater than a critical value n_a in terms of three smoothly joined parabolas in the square root of the density, so that in the limit of infinite compression it increases linearly with density. In the

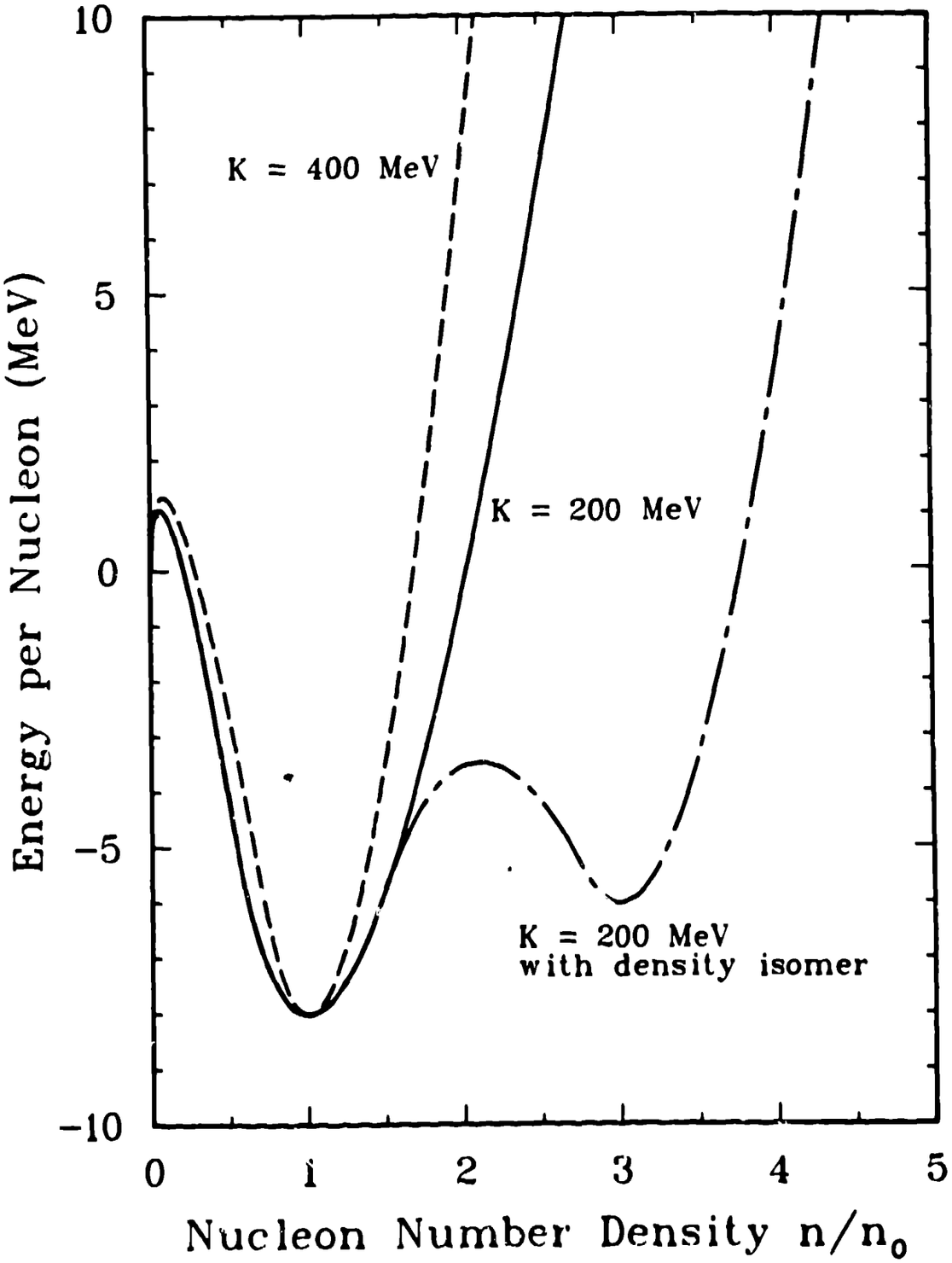

Fig. 2. Compressional contribution to our three nuclear equations of state.

limit of zero density, $E_0(n)$ is taken to be the difference between a specified term proportional to $n^{2/3}$ that represents the kinetic energy of noninteracting nucleons and a term proportional to n whose coefficient is adjusted so that the two forms join smoothly with continuous value and first derivative.

3. Relativistic Nuclear Fluid Dynamics

In order for conventional relativistic nuclear fluid dynamics to be a valid description[1] of high-energy heavy-ion collisions, there must be (1) a large number of degrees of freedom, (2) sufficient time during the collision to establish local equilibrium, and (3) a short mean free path for stopping a nucleon. The first condition is satisfied moderately well and the second condition is satisfied less well, but perhaps well enough. The third condition is more subtle, since estimates based on free nucleon-nucleon collisions give relatively long mean free paths[2-8] whereas coherent collective-field effects could in principle reduce the mean free path significantly.[11] The applicability of conventional relativistic nuclear fluid dynamics to high-energy heavy-ion collisions is an important question that must be decided from comparisons with experimental data rather than from theoretical arguments.[9] This is one of our purposes here.

In a complete nuclear fluid-dynamics calculation, we would need to take into account nuclear energy, Coulomb energy, nuclear viscosity, thermal conductivity, and single-particle effects, as well as the production of additional particles and the associated radiative loss of energy from the system. However, in heavy-ion collisions at the laboratory bombarding energy per nucleon of 393 MeV considered here, these effects are small compared to those caused by the dominant kinetic, compressional, and thermal energies, and are consequently neglected.

The covariant relativistic hydrodynamic equations that we solve express the conservation of nucleon number, momentum, and energy, for a specified nuclear equation of state. In units in which the speed of light $c = 1$, these equations are[1]

$$\frac{\partial N}{\partial t} + \nabla \cdot (\vec{v}N) = 0 \ ,$$

$$\frac{\partial \vec{M}}{\partial t} + \nabla \cdot (\vec{v}\vec{M}) = -\nabla p \ ,$$

and

$$\frac{\partial E}{\partial t} + \nabla \cdot (\vec{v}E) = -\nabla \cdot (\vec{v}p) \ ,$$

where N, $\vec{M}$, and E are respectively the nucleon number density, momentum density, and energy density (including rest energy) in the laboratory reference frame and $\vec{v}$ is the velocity of matter relative to the laboratory frame. The three laboratory-frame quantities are related to rest-frame quantities by

$$N = \gamma n \ ,$$

$$\vec{M} = \gamma^2(\varepsilon + p)\vec{v} \ ,$$

and

$$E = \gamma^2(\varepsilon + p) - p \ ,$$

where $\gamma = (1 - v^2)^{-1/2}$ and ε is the internal energy density in the rest frame, which is related to the internal energy per nucleon of eq. (1) by

$$\varepsilon = [m_0 + E(n,I)]n \ .$$

For a given nuclear equation of state and for given initial conditions we solve these equations numerically in three spatial dimensions by use of an improved version[23] of a particle-in-cell finite-difference computing method.[12] This is done for the reaction $^{20}Ne + ^{238}U$ at a laboratory bombarding energy per nucleon of 393 MeV, for which there exist experimental data on the cross section $d^2\sigma/dEd\Omega$ for outgoing charged particles, both integrated over all impact parameters[25] and for high-multiplicity events that can be tentatively identified with nearly central collisions.[29,30] For each of the three equations of state illustrated in fig. 2, we solve the equations of motion for five different impact parameters. We continue calculating the fluid-dynamical expansion to relatively small densities, where

the thermal energy per nucleon is negligible, rather than perform a thermal folding after the system reaches a freezeout density at which fluid dynamics ceases to be valid.[17]

We show in fig. 3 the calculated time evolution of the matter distribution for an impact parameter that is 0.1 the sum of the target and projectile radii, corresponding to nearly central collisions. Each column presents a side view of the matter distribution evolving in time for a different equation of state. The initial frame in each case shows a ^{238}U target bombarded from above by a Lorentz-contracted ^{20}Ne projectile whose energy per nucleon is 393 MeV. The projectile and target are represented by computational particles, which are initially aligned so that in the direction perpendicular to the page only a single point is visible. However, as the impulse resulting from the collision propagates throughout the system this alignment is destroyed and additional particles come into view.

The target and projectile are initially deformed, compressed, and excited by the collision, which produces curved shock waves. These are followed by rarefaction waves and an overall expansion of the matter into a moderately wide distribution of angles. The results for the three different equations of state are very similar to one another, but the expansion starts later because the matter is compressed to a higher density for our equation of state with a density isomer compared to our two conventional equations of state. In particular, for our equation of state with a density isomer the matter is compressed to a maximum rest-frame density of 5.1 n_0 and remains above about 3 n_0 for 1.4×10^{-22} s and above 2 n_0 for 1.9×10^{-22} s. For our conventional equation of state with compressibility coefficient K = 200 MeV, the matter is compressed to a maximum rest-frame density of 3.9 n_0 and remains above 2 n_0 for 1.0×10^{-22} s. For our conventional equation of state with K = 400 MeV, the matter is compressed to a maximum rest-frame density of 3.4 n_0 and remains above 2 n_0 for 0.7×10^{-22} s.

4. Comparison with Experimental Data

For a given impact parameter we construct from the velocity vectors at some large time the energy and angular distributions for the expanding matter. The small amount of matter that already has passed through the top and side boundaries of the computational mesh is also included. By integrating over the appropriate ranges of impact parameter, we compute the double-differential cross section corresponding both to all impact

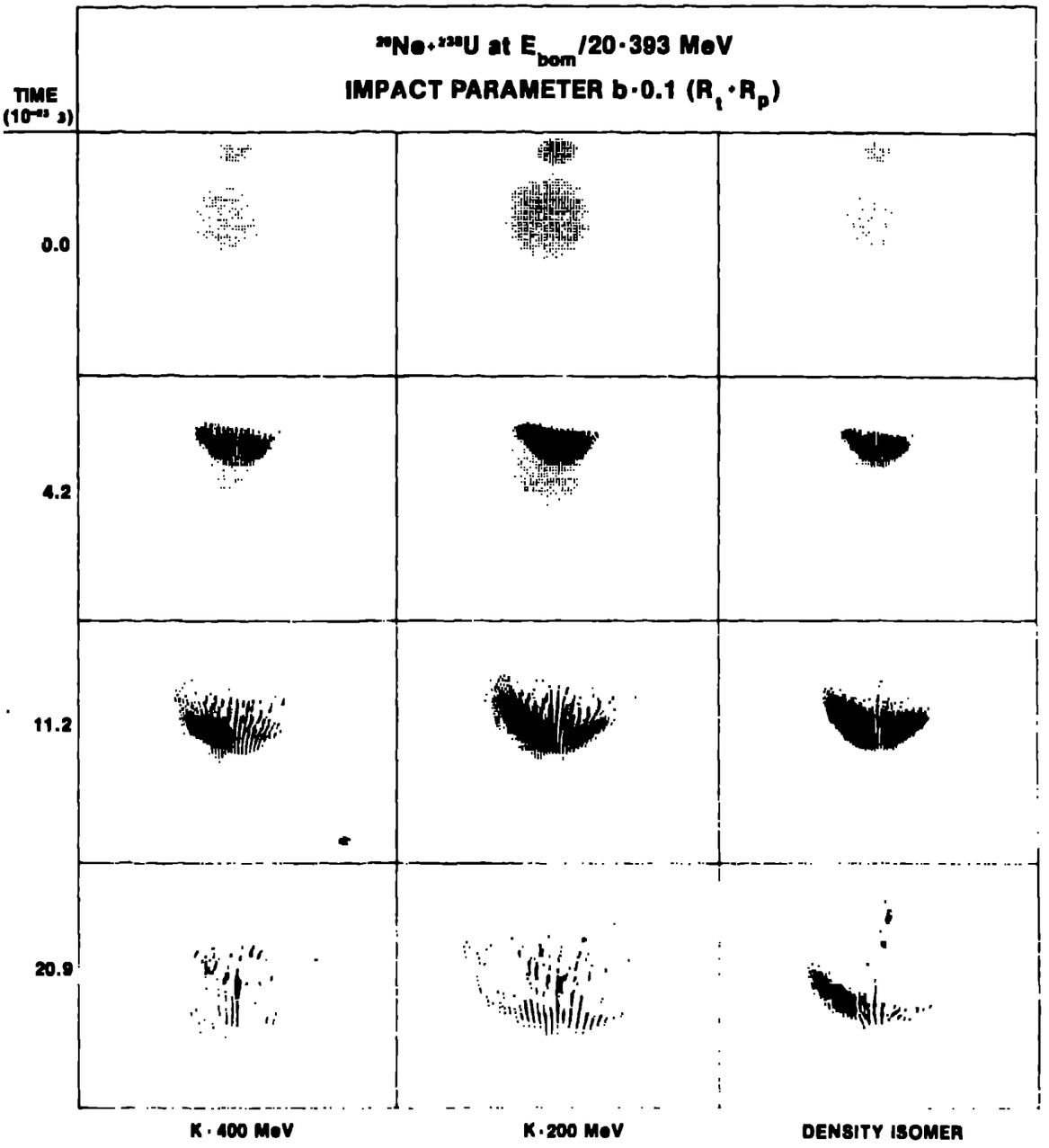

Fig. 3. Time evolution of the matter distribution in a nearly central collision of ^{20}Ne with ^{238}U, calculated for three different nuclear equations of state.

parameters and to central collisions constituting 15% of the total cross section. The cross section for the outgoing matter distribution is then converted into the cross section $d^2\sigma/dE d\Omega$ for outgoing charged particles under the assumption of uniform charge density.

The results calculated for our three equations of state are shown in figs. 4-6 in the form of energy spectra at four laboratory angles ranging from 30° to 150°. Some measure of the fairly large numerical inaccuracies inherent in fluid-dynamics calculations can be determined from the fluctuations in the histograms, which are obtained using angular bins of 10° width. We also include in the figures the experimental data for outgoing charged particles. The data of Sandoval et al.[25] for all impact parameters include contributions from protons, deuterons, tritons, ^{3}He particles, and ^{4}He particles. The data of Stock et al.[29,30] for high-multiplicity events, which are presumably associated with nearly central collisions, include contributions from only protons, deuterons, and tritons.

Examining first the results for all impact parameters given in the left-hand sides of figs. 4-6, we see that at low energy the calculated results are for all angles and equations of state higher than the experimental results. This is because of our neglect of binding, which causes the entire system to completely disintegrate into slowly moving matter for an arbitrarily small impulse. At higher energy the calculations with all equations of state reproduce, to within numerical uncertainties, the experimental data at all angles. The nuclear equation of state has little effect on the single-particle-inclusive cross section $d^2\sigma/dE d\Omega$ integrated over all impact parameters.

Turning now to the results for central collisions given in the right-hand sides of figs. 4-6, we see that at intermediate angles the results calculated with the three equations of state are very similar to one another, to within numerical uncertainties. However, at $\theta = 30°$ the slope of the energy spectrum decreases significantly as we go from a stiff equation of state with $K = 400$ MeV through an intermediate one with $K = 200$ MeV to a soft one that contains a density isomer. Also, at $\theta = 150°$ the results calculated for the density isomer are somewhat higher than those calculated for the two conventional equations of state. These differences arise because the softer density-isomer equation of state leads to higher initial density and thermal energy per nucleon, which increases the thermal contribution to the cross section in regions where it would otherwise be small.

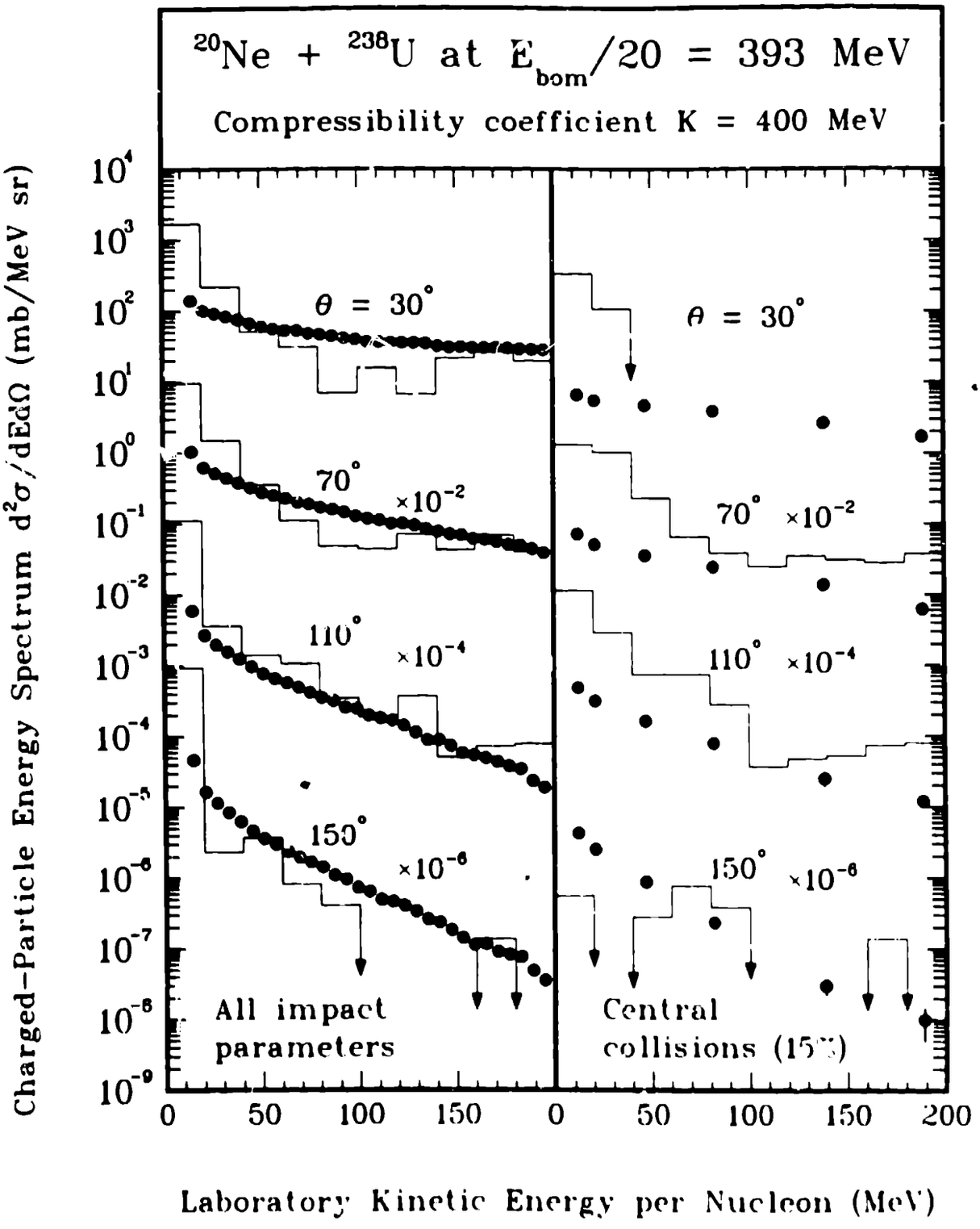

Fig. 4. Comparison of experimental energy spectra[5,9,10] with histograms calculated for our conventional nuclear equation of state with compressibility coefficient K = 400 MeV.

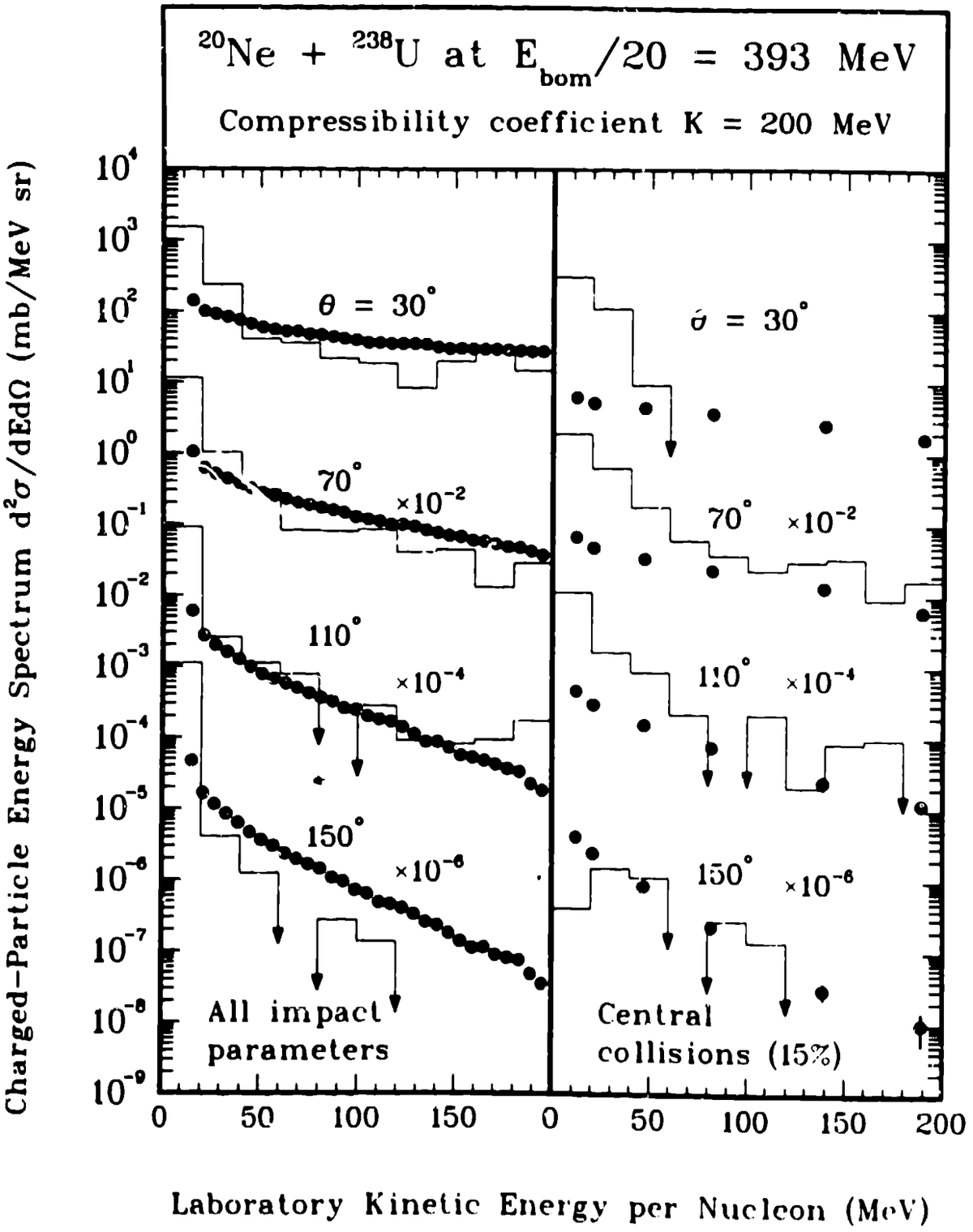

Fig. 5. Comparison of experimental energy spectra[25,29,30] with histograms calculated for our conventional nuclear equation of state with compressibility coefficient K = 200 MeV.

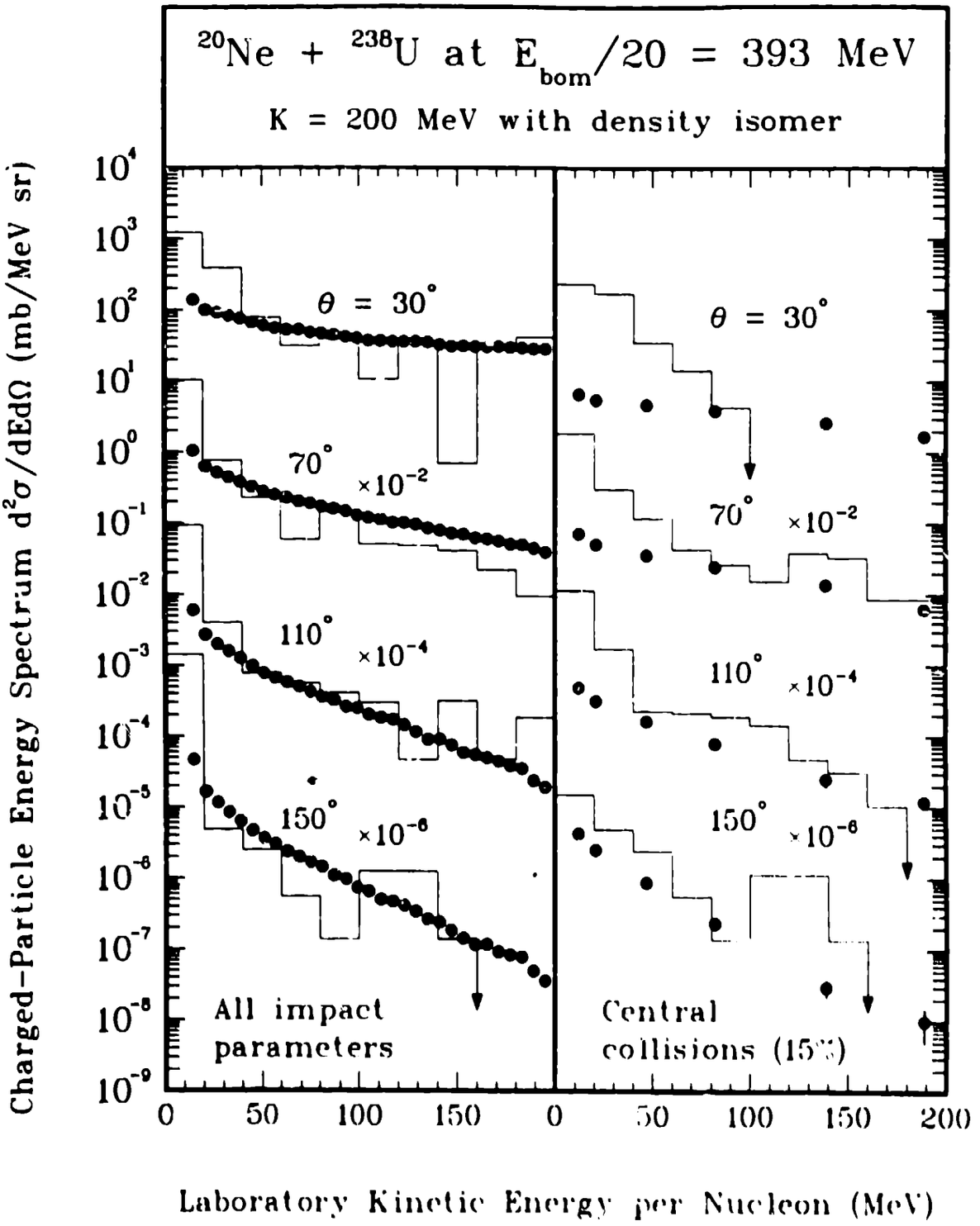

Fig. 6. Comparison of experimental energy spectra[illegible] with histograms calculated for our nuclear equation of state with a density isomer.

Because of our neglect of binding, at low energy the calculated results for central collisions are also higher than the experimental results for all angles and equations of state except for $\theta = 150°$ with the two conventional equations of state, where the rapid expansion in the backward direction suppresses the cross section. At higher energy the calculations with all equations of state reproduce, to within numerical uncertainties, the experimental data at all angles except $\theta = 30°$, where the calculated energy spectra for all three equations of state have significantly larger slopes than the experimental spectrum. This important discrepancy for central collisions in the forward direction suggests one or more of the following possibilities: (1) an experimental contamination from large impact parameters, (2) a direct component involving single-nucleon scattering, (3) a high-temperature thermal component, (4) a soft nuclear equation of state, or (5) interpenetration of the target and projectile upon contact. It is this latter possibility that we regard as most likely and to which we now turn our attention.

5. Interpenetration of Target and Projectile

In microscopic approaches such as the intranuclear cascade,[11] the target and projectile interpenetrate upon contact by amounts determined by a superposition of individual hadron-hadron collisions. An alternative way to incorporate target and projectile interpenetration while retaining some degree of coherent collective flow is by use of a two-fluid model,[2] in which coupled relativistic equations of motion are solved for separate target and projectile nuclear fluids. The terms in the equations that couple the two nuclear fluids are obtained from the cross section and mean longitudinal momentum transfer for free nucleon-nucleon collisions. At low relative velocities the target and projectile fluids merge, in which case conventional relativistic one-fluid dynamics is recovered.

For our calculations with the two-fluid model, we use an older nuclear equation of state in which the ground-state energy is of the form[10]

$$\epsilon_0(n) = an^{2/3} - bn + cn^{5/3} ,$$

with values of the constants that lead to a nuclear compressibility coefficient

$K = 294.8$ MeV .

For consistency, we also use this same equation of state in those calculations with our one-fluid model that are reported in this section.

We show in fig. 7 the resulting energy spectra calculated for central collisions in both the one-fluid and two-fluid models, along with the experimental data of Stock et al. For the three angles $\theta = 70°$, 110°, and 150°, the two models reproduce equally well, to within numerical uncertainties, the experimental data at high energy and are both larger than the experimental data at low energy because of our neglect of binding. For $\theta = 30°$, the two-fluid model agrees with the experimental data substantially better than does the one-fluid model, although the slope calculated from the two-fluid model is still somewhat larger than the experimental slope.

An alternative and perhaps more illuminating way of making the comparisons for central collisions is in the form of angular distributions for fixed outgoing laboratory momentum per nucleon, as shown in fig. 8. The experimental angular distributions for low outgoing momenta contain a small peak that shifts to smaller angles and finally disappears for higher outgoing momenta. The histograms are calculated with energy bins of 20 MeV. Because of our neglect of binding, the results for the lowest outgoing momentum calculated in both the one-fluid and two-fluid models are much larger than the experimental data. With increasing outgoing momentum, the one-fluid model predicts angular distributions that are narrower than the experimental distributions and that are peaked at increasingly larger angles, which is opposite to the experimental trend. However, the two-fluid model predicts angular distributions with peaks that shift to smaller angles with increasing outgoing momentum, as is observed experimentally. For intermediate outgoing momenta the experimental data are lower in absolute value than the two-fluid calculations, but for the two highest outgoing momenta the experimental data agree with the two-fluid calculations to within their numerical uncertainties.

6. Conclusions

By focussing in figs. 7 and 8 on those regions in energy and angle that are sensitive to the model used, namely high-energy outgoing particles in forward directions resulting from central collisions, we conclude that conventional nuclear fluid dynamics is inadequate and that the

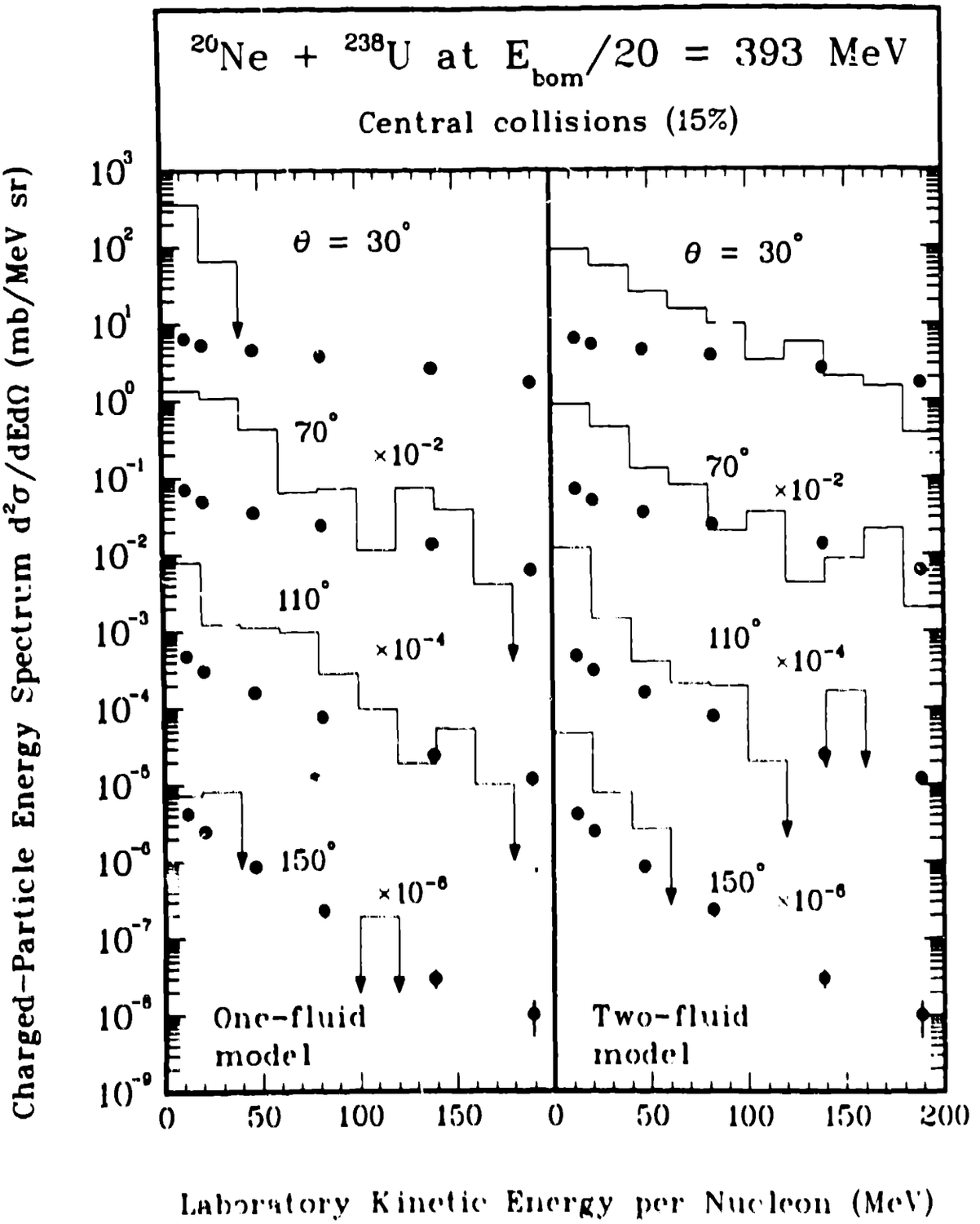

Fig. 7. Comparison of experimental energy spectra for central collisions[9,10] with histograms calculated in the one-fluid and two-fluid models.

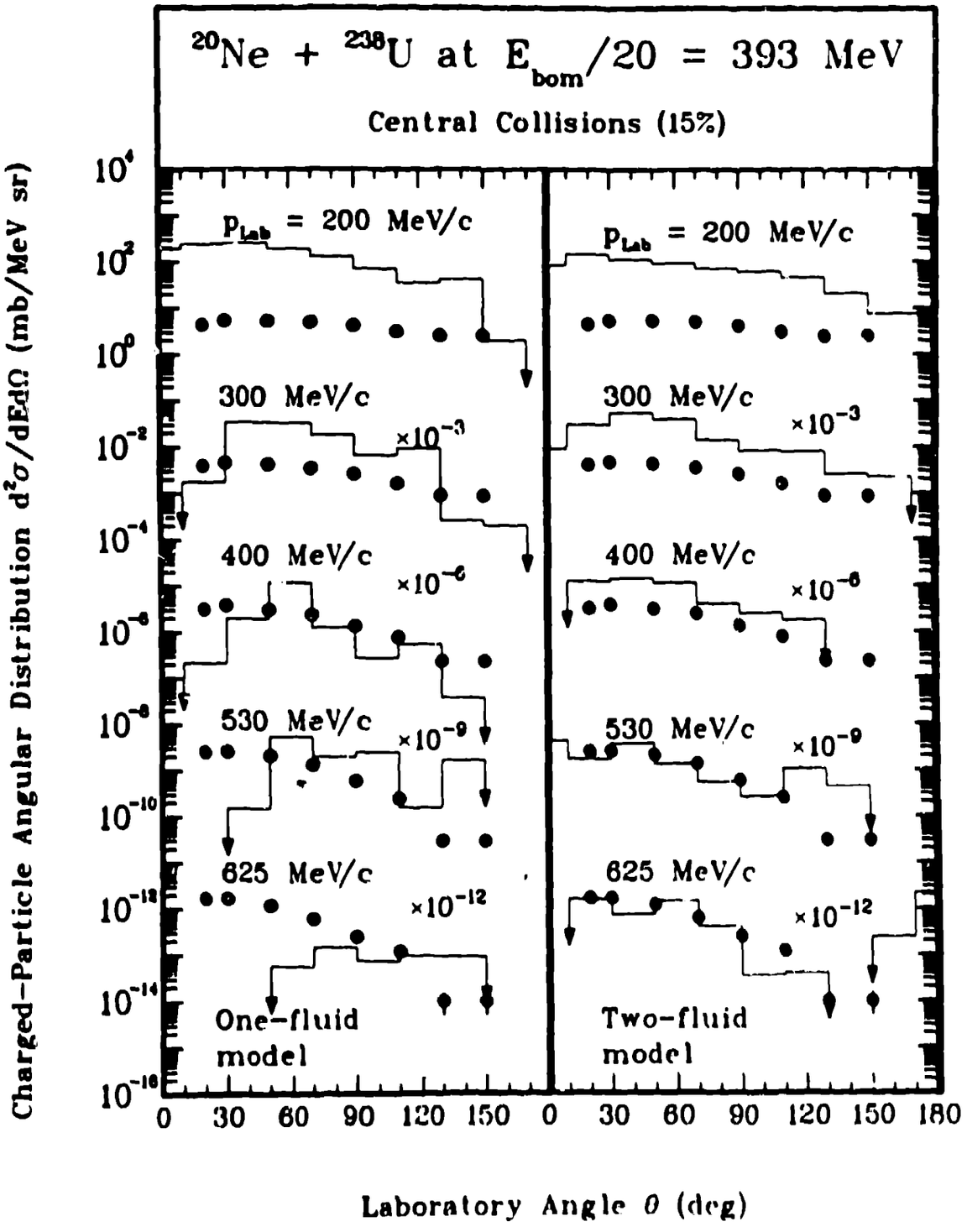

Fig. 8. Comparison of experimental angular distributions for central collisions[9,10] with histograms calculated in the one-fluid and two-fluid models.

interpenetration of the target and projectile upon contact must be taken into account. The two-fluid model that is used here to describe this interpenetration predicts sidewards peaking for central collisions that is in approximate agreement with experimental results, although for intermediate outgoing momenta the calculated peak is somewhat higher than the experimental peak. In contrast, the microscopic intranuclear-cascade calculations of Yariv and Fraenkel,[31,32] which are based on a superposition of hadron-hadron collisions, predict for central collisions angular distributions at all outgoing momenta that are forward peaked, to within statistical errors. Furthermore, the two-component direct-plus-thermal model of Schürmann and Chemtob[26,27] yields for central collisions angular distributions that are forward peaked at low and intermediate outgoing momenta and slightly sidewards peaked at higher outgoing momenta. From this we conclude that central high-energy heavy-ion collisions involve some degree of coherent collective flow rather than being merely a superposition of hadron-hadron collisions In particular, the flow appears to be somewhat intermediate between that of two-fluid dynamics and an intranuclear cascade.

From figs. 4-6 we see that, apart from central collisions at $\theta = 30°$ and to a less extent 150°, the double differential cross section $d^2\sigma/dEd\Omega$ is relatively insensitive to the nuclear equation of state in one-fluid dynamics, and we expect even less sensitivity in two-fluid dynamics. However, as stressed by Buchwald et al.[6] and Csernai et al.,[8] the triple differential cross section $d^3\sigma/dEd\theta d\phi$ should be more sensitive. This is because for a given impact parameter that is intermediate between central and peripheral, the mean angles of the emitted projectile-like and target-like matter depend upon the maximum density reached and the time that the system remains compressed and consequently upon the nuclear equation of state. With the experimental development of 4π detectors in the near future, the exploration of this new possibility should become a reality.

Other promising directions that deserve further studies include charged pion spectra, two-particle correlations, composite-particle production, and anomalously short mean free paths of projectile fragments.[10] Learning whether or not the nuclear equation of state contains any surprises represents an important challenge, but this will require more precise experiments and theory and the development of a clearer signature.

We are grateful to R. Stock, Y. Yariv, Z. Fraenkel, and B. Schürmann for enlightening discussions and for providing us with their experimental data and theoretical calculations prior to publication. This work was supported by the Alexander von Humboldt Foundation and the U.S. Department of Energy.

References

1. Amsden, A. A., Harlow, F. H., and Nix, J.R. (1977), Relativistic Nuclear Fluid Dynamics, Phys. Rev. C15, 2059-2071.
2. Amsden, A. A., Goldhaber, A. S., Harlow, F. H., and Nix, J. R. (1978), Relativistic Two-Fluid Model of Nucleus-Nucleus Collisions, Phys. Rev. C17, 2080-2096.
3. Baym, G. and Chin, S. A. (1976), Can a Neutron Star Be a Giant MIT Bag?, Phys. Lett. 62B, 241-244.
4. Blaizot, J. P., Gogny, D., and Grammaticos, B. (1976), Nuclear Compressibility and Monopole Resonances, Nucl. Phys. A265, 315-336.
5. Brown, G. E. and Weise, W. (1976), Pion Condensates, Phys. Rep. 27C, 1-34.
6. Buchwald, G., Csernai, L. P., Maruhn, J. A., Greiner, W., and Stöcker, H. (1980), Importance of Nuclear Viscosity and Thermal Conductivity and the Analysis of the Bounce-Off Effect in High Energy Heavy Ion Collisions, University of Frankfurt Preprint UFTP 42/1980.
7. Chapline, G. and Nauenberg, M. (1977), Asymptotic Freedom and the Baryon-Quark Phase Transition, Phys. Rev. D16, 450-456.
8. Csernai, L. P., Subramanian, P. R., Buchwald, G., Graebner, G., Kruse, H., Maruhn, J. A., Stöcker, H., and Greiner, W. (1980), Nuclear Chemistry in the Evaporation Following the Fluid Dynamical Flow in Energetic Heavy Ion Reactions, University of Frankfurt Preprint UFTP 37/1980.
9. Friar, J. L. and Negele, J. W. (1975), Theoretical and Experimental Determination of Nuclear Charge Distributions, Adv. Nucl. Phys. 8, 219-376.
10. Friedlander, E. M., Gimpel, R. W., Heckman, H. H., Karant, Y. J., Judek, B., and Ganssauge, E. (1980), Evidence for Anomalous Nuclei among Relativistic Projectile Fragments from Heavy-Ion Collisions at 2 GeV/Nucleon, Phys. Rev. Lett. 45, 1084-1087.

11. Gyulassy, M. and Greiner, W. (1977), Critical Scattering and Pionic Instabilities in Heavy Ion Collisions, Ann. Phys. (N.Y.) 109, 485-527.
12. Harlow, F. H., Amsden, A. A., and Nix, J. R. (1976), Relativistic Fluid Dynamics Calculations with the Particle-in-Cell Technique, J. Comp. Phys. 20, 119-129.
13. Hecking, P. and Weise, W. (1979), Pion Condensation and Density Isomerism in Nuclear Matter, Phys. Rev. C20, 1074-1078.
14. Irvine, [illegible] (1975), Pion Condensation and Other Abnormal States of Matter, Rep. Prog. Phys. 38, 1385-1425.
15. Keister, B. D. and Kisslinger, L. S. (1976), Free-Quark Phases in Dense Stars, Phys. Lett. 64B, 117-120.
16. Lee, T. D. (1975), Abnormal Nuclear States and Vacuum Excitation, Rev. Mod. Phys. 47, 267-275.
17. Mekjian, A. (1977), Thermodynamic Model for Composite-Particle Emission in Relativistic Heavy-Ion Collisions, Phys. Rev. Lett. 38, 640-643.
18. Möller, P. and Nix, J. R. (1981), Nuclear Mass Formula with a Yukawa-plus-Exponential Macroscopic Model and a Folded-Yukawa Single-Particle Potential, Nucl. Phys., in press.
19. Myers, W. D. and Swiatecki, W. J. (1969), Average Nuclear Properties, Ann. Phys. (N.Y.) 55, 395-505.
20. Myers, W. D. (1976), Development of the Semiempirical Droplet Model, At. Data Nucl. Data Tables 17, 411-417.
21. Negele, J. W. and Rinker, G. (1977), Density-Dependent Hartree-Fock Description of Nuclei in the Rare Earth and Nickel Regions, Phys. Rev. C15, 1499-1514.
22. Nix, J. R. (1979), Theory of High-Energy Heavy-Ion Collisions, Prog. Part. Nucl. Phys. 2, 237-284.
23. Nix, J. R. and Strottman, D. (1981), Effect of a Density Isomer on High-Energy Heavy-Ion Collisions, Phys. Rev. C, in press.
24. Nyman, E. M. and Rho, M. (1976), Abnormal Nuclear Matter and Many-Body Forces, Nucl. Phys. A268, 408-444.
25. Sandoval, A., Gutbrod, H. H., Meyer, W. G., Stock, R., Lukner, C., Poskanzer, A. M., Gosset, J., Jourdain, J. C., King, C. H., King, G., Nguyen, V. S., Westfall, G. D., and Wolf, K. L. (1980), Spectra of p, d, and t from Relativistic Nuclear Collisions, Phys. Rev. C21, 1321-1343.

26. Schürmann, B. and Chemtob, M. (1980), Direct Versus Thermal Particle Emission in High-Energy Heavy-Ion Collisions: Multiplicity-Selected Proton Inclusive Spectra, Z. Phys. A294, 371-376.
27. Schürmann, B. (1981), private communication.
28. Sobel, M. I., Siemens, P. J., Bondorf, J. P., and Bethe, H. A. (1975), Shock Waves in Colliding Nuclei, Nucl. Phys. A251, 502-529.
29. Stock, R., Gutbrod, H. H., Meyer, W. G., Poskanzer, A. M., Sandoval, A., Gosset, J., King, C. H., King, G., Lukner, C., Nguyen, V. S., Westfall, G. D., and Wolf, K. L. (1980), Emission Patterns in Central and Peripheral Relativistic Heavy-Ion Collisions, Phys. Rev. Lett. 44, 1243-1246.
30. Stock, R. (1981), private communication.
31. Yariv, Y. and Fraenkel, Z. (1980), Intranuclear Cascade Calculation of High Energy Heavy Ion Collisions: Effect of Interactions Between Cascade Particles, Weizmann Institute of Science Preprint WIS-18/80/Sept.-ph.
32. Yariv, Y. and Fraenkel, Z. (1981), private communication.